Holocene dynamics of the salt-fresh groundwater interface under a sand island, Inhaca, Mozambique

4 authors, including:

L. Vaeret
Independent Researcher

6 PUBLICATIONS   **64** CITATIONS

SEE PROFILE

Anton Leijnse
Wageningen University & Research

91 PUBLICATIONS   **1,244** CITATIONS

SEE PROFILE

Sylvi Haldorsen
Norwegian University of Life Sciences (NMBU)

58 PUBLICATIONS   **695** CITATIONS

SEE PROFILE

Some of the authors of this publication are also working on these related projects:

Project   International Union of Geological Sciences View project

Project   International Geoscience Program (IGCP-618) View project

Holocene dynamics of the salt–fresh groundwater interface under a sand island, Inhaca, Mozambique

Lars Været [a,*], Anton Leijnse [b], Fortunato Cuamba [c], Sylvi Haldorsen [a]

[a] Department of Plant and Environmental Sciences, Norwegian University of Life Sciences, P.O. Box 5003, N 1432 Aas, Norway
[b] Department of Environmental Sciences; Soil Physics, Ecohydrology and Groundwater Management Group, Droevendaalsesteeg 4, P.O. Box 47, 6700 AA, Wageningen, The Netherlands
[c] Department of Geology, University of Eduardo Mondlane, Mozambique

ARTICLE INFO

ABSTRACT

The configuration of coastal groundwater systems in southeast Africa was strongly controlled by the Holocene sea-level changes, with an Early Holocene transgression ~15 m (10,000–5000 cal BP), and two assumed high-stand events in the Middle and Late Holocene with levels higher than the present. The fluctuation of the salt–fresh groundwater interface under Inhaca Island in Mozambique during the Holocene has been studied using an adapted version of the numerical code SUTRA (**S**aturated-**U**nsaturated **Tra**nsport). In this study, small-scale variations such as tidal effects have not been considered. A number of transient simulations were run with constant boundary conditions until the steady state condition was reached in order to study the sensitivity of response time, salt–fresh interface position, and thickness of the transition zone to different parameters such as hydraulic conductivity, porosity, recharge, and dispersivity. A 50% increase in horizontal hydraulic conductivity yields a rise in the location of the interface of >15 m, while an increase in recharge from 8% to 20% of mean annual precipitation (MAP) causes a downward shift in the interface position of >40 m. A full transient simulation of the Holocene dynamics of the salt–fresh groundwater interface showed a response time of several hundred years, with a duration sensitive to porosity, hydraulic conductivity and recharge and a position determined by the recharge rate and the hydraulic conductivity. Dispersivity controls the thickness of the transition zone in this non-tidal model. Physical processes, such as changes in recharge and/or the sea level, may cause rapid shifts in the interface position and affect the thickness of the transition zone.

© 2011 Elsevier Ltd and INQUA. All rights reserved.

1. Introduction

Climate fluctuations have forced sea-level fluctuations throughout geologic time, with a magnitude of ca 130 m during the Late Pleistocene and Holocene (Fleming et al., 1998; Lambeck and Chappell, 2001; Lambeck et al., 2002; Peltier, 2002). In addition, isostatic or tectonic depression and rise of continental plates have resulted in variable sea-level fluctuations worldwide. Ghyben (1888) and Herzberg (1901) were the first to describe how density differences between salt and fresh water determine the shape and position of the salt–fresh groundwater interface. Major shifts of the salt–fresh groundwater interface, and of the thickness of the fresh groundwater lens, have therefore taken place along the world's coastlines. The Ghyben–Herzberg relation assumes a sharp interface and a stagnant salt-water zone, which is not strictly true. Their theories only hold approximately if the fresh groundwater lens is in equilibrium with the present sea level and climate.

Several studies have focused on factors influencing the behaviour of the salt–fresh transition zone in coastal aquifers, including changes in the thickness and the position of the transition zone following from changes in base level (i.e. sea-level variations) (e.g. Meisler et al., 1984; Underwood et al., 1992; Essink, 1996; Kiro et al., 2008; Yechieli et al., 2010). Many of the studies also focus on the time involved for a new equilibrium to be established between the new base level (i.e. sea-level) and the interface position and/or transition zone thickness. Lambrakis and Kallergis (2001) and Lambrakis (2006) studied freshening times of coastal groundwater in Greece after it had first gone through salinization due to over-pumping.

Meisler et al. (1984) studied the effects of large-scale eustatic sea-level fluctuations on the seawater–freshwater interface along a cross section (240 km long) in the northern Atlantic Coastal Plain. A finite-difference computer model was developed to simulate

density-driven groundwater flow within the freshwater system for several static sea-level positions. A broad transition zone of 300–600 m was attributed to sea-level fluctuations over millions of years. The study concluded that the salt–fresh interface is not in equilibrium with present sea levels. This is in agreement with the conclusion by Essink (1996) who also found that a time lag between cause and effect can be expected to be a few centuries for small hydrogeologic systems (<10 km) such as an island. On a much smaller spatial scale, Underwood et al. (1992) studied factors influencing the behaviour of salt–fresh transition zones under atoll islands, using both a tidal and a non-tidal model approach. Underwood et al. (1992) found that the most important natural control of the transition zone thickness is vertical tidal variations, but found transverse dispersivity to be the decisive factor in their non-tidal model. Kiro et al. (2008) studied the effects of a drop in base level, using the Dead Sea as an example, one conclusion being that the longitudinal dispersivity causes a widening of the transition zone as the transition zone moves vertically during a change in lake level. The importance of geometry has been addressed by Yechieli et al. (2010), and their numerical simulations show that the response of the fresh–saline interface of groundwater systems to global sea-level rise depends on coastal topography next to the shoreline.

This study is focused on the seawater–freshwater interface of groundwater systems on the Inhaca Island, Mozambique (Fig. 1), related to Holocene sea-level fluctuations. These fluctuations have been incorporated into a groundwater model through time-dependent boundary conditions so that the dynamics of the salt–fresh groundwater interface, and possible time lags therein, can be studied. The primary objective has been to investigate long-term responses of the freshwater lens to sea-level variations over a time span of several millennia. Short term (<1 month) fluctuations, such as tidal movement, have therefore been ignored. The SUTRA code (**S**aturated-**U**nsaturated **Tra**nsport) (Voss and Provost, 2003) has been adapted for transient simulations of the seawater–freshwater interface, with the option of switching from pressure boundary condition to groundwater recharge and vice versa. The adapted code estimates the position of the interface and the thickness of the transition zone by calculating the spatial statistical moments of the vertical derivative of the concentration field.

The results are believed to be valid for many coastal islands in southern Africa, and also elsewhere where Holocene sea-level fluctuations have occurred. To the authors' knowledge, no similar long-term approach has been applied before, although several studies of shifts in the salt–fresh groundwater interface have been published (Meisler et al., 1984; Essink, 1996, 2001; Kooi et al., 2000; Lambrakis and Kallergis, 2001; Lambrakis, 2006).

2. Regional setting

2.1. Area description and present climate

Inhaca (47 km^2) is an island 35 km east of Maputo, Mozambique (Fig. 1). The island comprises two main vegetated coastal dune ridges stretching NNE–SSW. The one along the western shore reaches heights of about 60 m a.s.l., and the ridge along the eastern shore peaks up to 115 m a.s.l. Between these two dune ridges there is an undulating plain with lower dunes and small inter-dunal wetlands. The depth of the sea (Fig. 1) increases rapidly to the east of the island, while the average depth in the Maputo Bay to the west is less than 10 m, with large areas of seabed being exposed during low tide.

Inhaca has a subtropical climate with an annual average temperature of ∼23 °C. Mean annual precipitation is ca 900 mm/y with more than one third falling in January and February. Mean annual evaporation exceeds 1100 mm/year (evaporation data from the period 1954–2001).
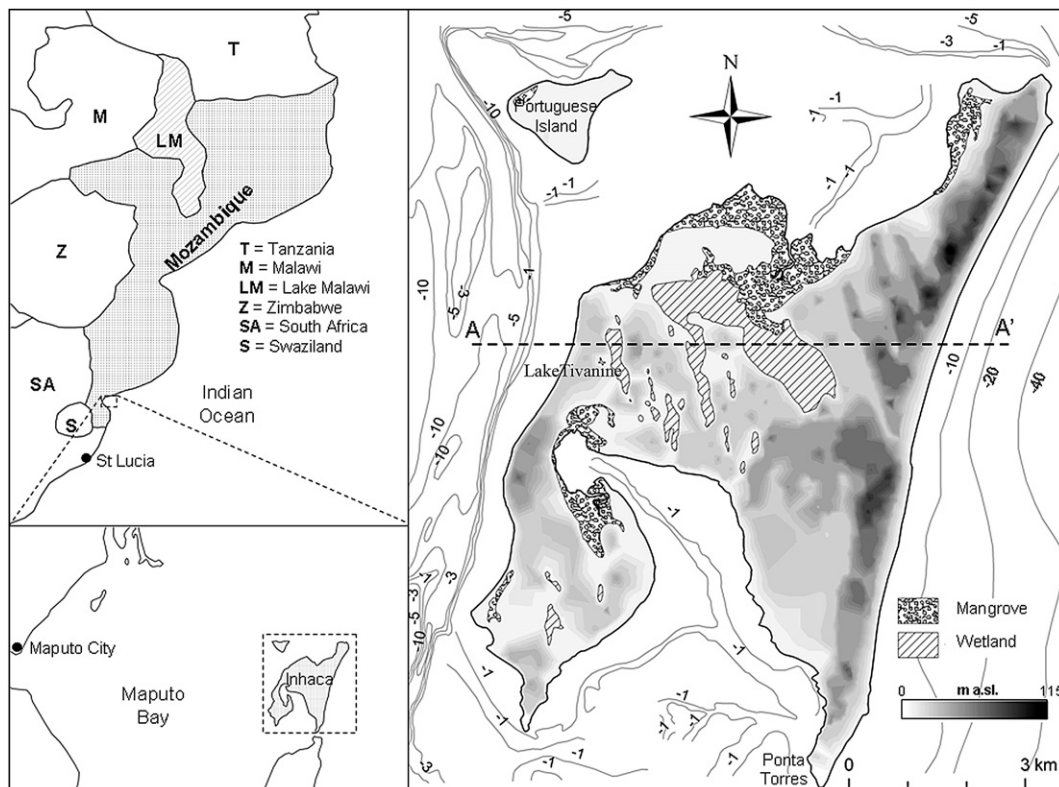

Fig. 1. Key map with the location of Inhaca Island in southern Mozambique.

Evergreen forest covers the tall dune ridges down to the sea. The undulating plain in the central part of the island has grassland and open evergreen bush land. The lower part of the wetlands is overgrown with freshwater-demanding reeds, while the drier bordering parts are cultivated. Mangroves fringe parts of the coastline (Fig. 1) (Kalk, 1995).

The change of landscape morphology in Inhaca during the Holocene is not taken into consideration in this study. In general, the main landscape elements are believed to be of pre-Holocene age (Sénvano et al., 1997).

2.2. Hydrogeology

Drilling of 8 wells in Inhaca showed aeolian sand from the surface to 30 m below the ground (Muianga, 1992), all assumed to be of Quaternary age (Sénvano et al., 1997). Little is known about the deeper and older geology, although observations at Ponta Torres (Fig. 1) suggested that the sand dunes overlie a base of calcareous sandstone (Hobday, 1977) most probably of Neogene age, as in other places in the Maputo District (Direcção Nacional de Geologia de Moçambique, 1995).

The groundwater level is below the ground surface in most of the wetlands, except during heavy rainfall and cyclonic events. The wetland sediments consist of 0.3–2 m thick peat, which commonly overlies aeolian or estuarine sand (Cuamba et al., 2007).

Palaeoclimate data from southern Africa displays a relationship between warm climate and wet conditions, while cooling is associated with drought (Partridge, 1997; Tyson, 1999; Tyson and Partridge, 2000; Holmgren et al., 2003). This applies to the scale of a glacial cycle, a millennium, as well as a few centuries. During the Last Glacial Maximum (LGM) (18–16,000 cal BP) the subcontinent was cooler and drier than today (Partridge, 1997; Partridge et al., 1999), but the temperature rose by 6–7 C° towards the Holocene Altithermal (7500–5100 cal BP), with an increase in annual rainfall up to 5–10 % above present (Partridge, 1997; Partridge et al., 1999; Scott and Lee-Thorp, 2004). The effect of temporary changes in vegetation has not been addressed specifically in this study.

2.3. Sea-level fluctuations and freshwater lens

The Holocene development of Maputo Bay (Fig. 2) has been reconstructed from the bathymetric data and the Holocene sea-level curve for southeast Africa (Ramsay, 1995). During the rapid sea-level rise in the Early Holocene the level reached −10 m around 10,000 cal BP (Ramsay and Cooper, 2002). For profile A–A′ in Fig. 1 a sea-level rise from −10 m at 10,000 cal BP to the present level at around 7400 cal BP (Fig. 2) would have reduced the total recharge of Inhaca by >30% due to a gradual reduction in area above sea level. Most of this reduction took place on the western side of the island, where the surface gradient is gentler than in the east.

Ramsay (1995) found a mid-Holocene (5000 cal BP) marine high stand of ∼3.5 m. The low-lying wetland areas in central Inhaca have an elevation of only 1–2 m a.s.l., and were probably flooded during the transgression towards this sea-level maximum. This is supported by the occurrence of up to 6 m thick sediments with marine and estuarine diatoms and bivalves under peat in the present freshwater swamp of Lake Tivanine (Fig. 1) (Cuamba et al., 2007), and by the development of a Holocene palaeotidal flat in the central area of Inhaca (Sénvano et al., 1997). A high stand of around 3 m would not only have reduced the recharge area, but would also have caused a dramatic shift in the position of discharge boundaries. In addition to this, a marine flooding of central Inhaca would
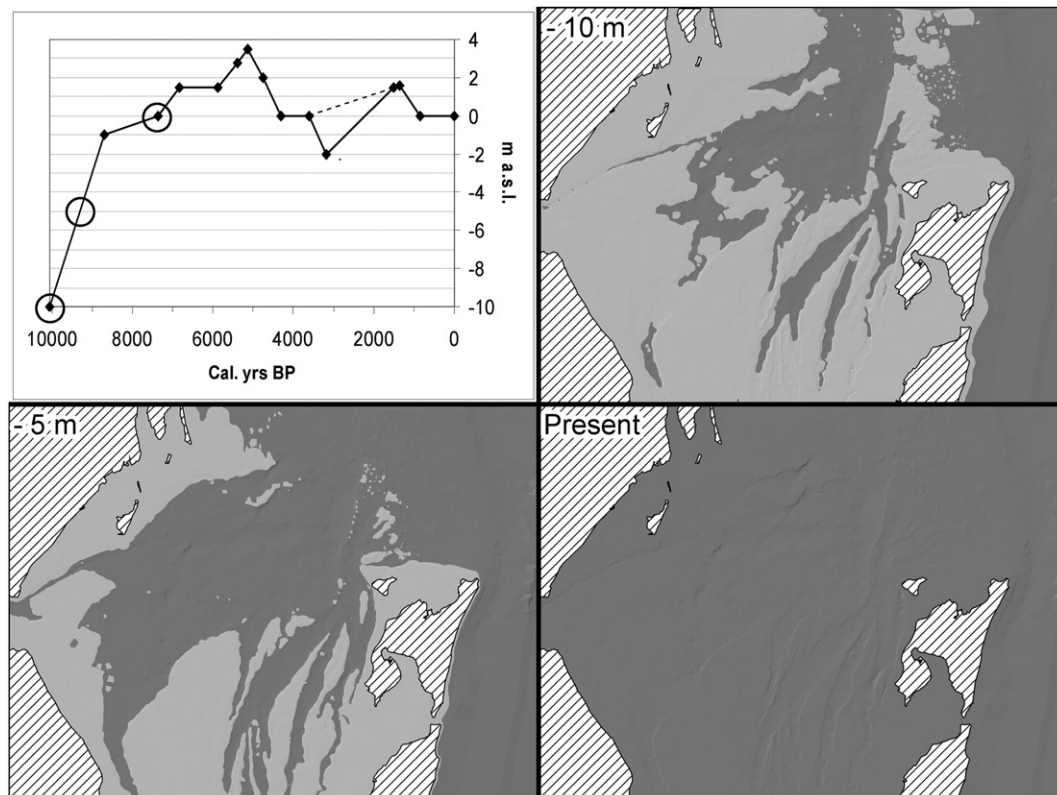

Fig. 2. Reconstruction of the Maputo Bay based on bathymetric map (Ministério de Defesa Nacional, 1985) and the Holocene sea-level curve (Ramsay, 1995) for three different sea-levels. Diagonal lines: present land surface. Light grey: dry land in Maputo Bay. Dark grey: sea.

have reduced the volume of the fresh groundwater lens considerably. The opposite effect of the 5–10 % higher than present rainfall, simulated by Partridge (1997) for the same period, is believed to be negligible in this setting. For this reason, and due to the low resolution of palaeorainfall data, Holocene variation in rainfall has been ignored in this study. Ramsey (1995) indicated a second marine high stand in the Late Holocene of about 1.5 m around 1500 cal BP (see Fig. 2), which ended ∼800 cal BP. Afterwards, relatively stable sea-level conditions have prevailed. The last high stand is included in the groundwater simulations although it is not as well documented as the one in the Middle Holocene.

3. Materials and methods

Numerical simulations were performed for a simplified two-dimensional cross section using an adapted version of the finite element code SUTRA (Voss and Provost, 2003). The model included

i) time-dependent boundary conditions and sources and sinks through independent input files and
ii) calculation of spatial statistical moments of the concentration field to characterize the transition zone over time

The input files to SUTRA, apart from the moment input file and time dependency input files, were generated using the graphical user interface (GUI) SutraGUI (Winston and Voss, 2004) that is designed to run with the ArgusONE™ package, and which provides 2D Graphical Information Systems (GIS) and meshing support.

A time-dependent sea-level boundary condition was used. For nodes with vertical coordinates lower than sea level, a prescribed pressure is assumed, with the pressure being determined by the reference pressure at sea level, and a hydrostatic pressure distribution below sea level. For nodes above sea level, a freshwater influx is assumed.

Spatial statistical moments of the vertical derivative of the concentration (C) field were calculated along vertical lines distributed along the length of the cross section (Fig. 3).

The moments are defined as (Govindaraju and Das, 2007):

0th moment:

$$M_0 = \int_y \frac{\partial C}{\partial y} dy \tag{1}$$

1st moment:

$$M_{1y} = \int_y \frac{\partial C}{\partial y} y \, dy \tag{2}$$

Considering the derivative of the salt concentration with depth to be a probability density function (PDF), the scaled first moment that follows from (1) and (2) is then given by:

$$\bar{y} = \frac{M_{1y}}{M_0} \tag{3}$$

This first scaled moment, or centre of mass is the mean of the PDF. If the salt concentration with depth would be symmetric, this is the depth where the derivative of the salt concentration is at its maximum, and the salt concentration itself is at 50% of the seawater concentration. For the dispersive system, although no salt–fresh interface exists, the first scaled moment is used as an approximation of the vertical position of the interface between salt and fresh water. It has been shown (Eeman et al., 2011) that this is a good approximation, even for salt concentration distributions that are not completely symmetric.

The 2nd central moment of the PDF is defined by:

$$M_{2yy} = \int_y \frac{\partial C}{\partial y} (y - \bar{y})^2 dy \tag{4}$$

and the variance follows from:

$$\sigma_{yy}^2 = \frac{M_{2yy}}{M_0} \tag{5}$$

Twice the standard deviation, σ_{yy}, is used as a measure of the thickness of the transition zone between salt and fresh water. If the
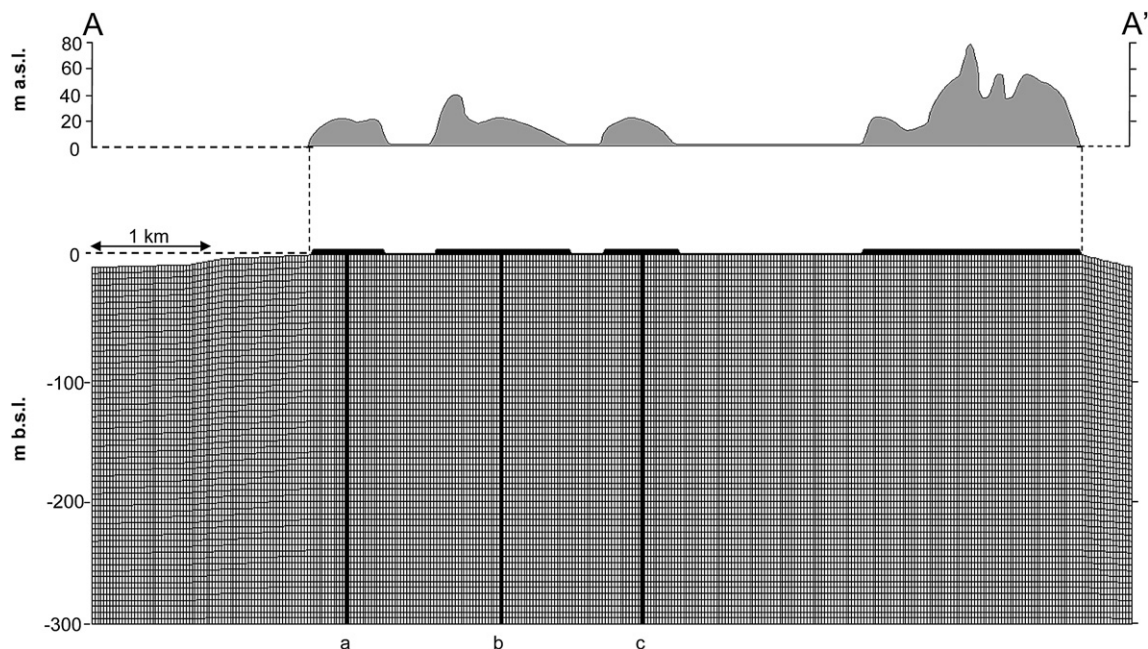

Fig. 3. Model domain represented by a deformable grid of quadrilaterals. Spatial statistical moments of the concentration field were calculated along the lines a, b and c.

Table 1
The range of parameter value input that have been used in the different simulations.

	Value	Units
Porosity, n	0.30–0.42	–
Horizontal K, K_{hor}	12–18	m/day
Vertical K, K_{ver}	2.5–3.5/10.5	m/day
Recharge	0.002–0.005 (8–20% of MAP)	m/day
Longitudinal dispersivity, α_L	15–30	m
Transverse dispersivity, α_T	1.5–3	m

Table 2
Combination of parameter values that generated the best fit to the analytical solution for interface position (Fig. 4).

Parameter	Value	Units
Porosity	0.42	–
K_{hor}/K_{ver}	18/3.5	m/day
Recharge	0.002 (8% of MAP)	m/day
α_L/α_T	15/1.5	m

salt concentration distribution were to be completely symmetric, twice the standard deviation would give the distance between the 16 and 84 percentile.

A single aquifer set-up was used according to the conceptual model described earlier. A grid of deformed quadrilaterals was used to represent a vertical cross section of the Inhaca Island (Fig. 3) from the Maputo Bay to the Indian Ocean along the line A–A′ shown in Fig. 1. The total distance is ∼8700 m while the distance from the top (+3.5 m a.s.l.) to the bottom of the domain was set to ∼300 m. An average size of 25 × 5 m was used for elements below the present sea level. Denser vertical element spacing was applied above the present sea level in order to be able to redefine nodes from specified pressure to source of fluid and vice versa, reflecting the same order of magnitude as experienced for sea-level variations during the Middle to Late Holocene.

The estimates of average recharge, permeability and porosity (Table 1) are based on literature data (Bredenkamp et al., 1993; Meyer and Godfrey, 1995; Schwartz and Zhang, 2003; Hiscock, 2005), instrumental records (precipitation data), and field data (grain-size distribution). Grain-size analyses of sediments from the saturated zone show well-sorted fine to medium sand, and porosity values of 30–42% have been applied in the model. This is within the range presented by Schwartz and Zhang (2003) for similar sediments. Hydraulic conductivity (K) has been estimated using the empirical Hazen's formula (Hazen, 1911) which relates grain size property d_{10} to K for sediments samples having a uniformity coefficient $d_{60}/d_{10} < 5$. For the grain size samples in this study this method indicates K-values of typically ∼3–20 m/day. The hydraulic conductivities of the calcareous sandstones that are assumed to underlie the island (Hobday, 1977) are in other areas found to be in the same range as the K-values of the unconsolidated sediments on Inhaca (Fish, 1988; Fish and Stewart, 1991). Therefore, it is appropriate to assume the entire model domain as homogeneous.

At 10,000 cal BP the transition zone did not instantaneously reach equilibrium after the preceding rapid sea-level rise. To use the steady state as an initial condition for the transient model, a few hundred years was simulated to reach equilibrium with sea-level 10,000 cal BP. After this adjustment, the simulated rate of change was kept constant for ∼2000 years until present sea level was reached ∼7400 cal BP, after which the rate of sea-level rise again changed.

Longitudinal (α_L) and transverse (α_T) dispersivity were applied to account for intrinsic inhomogeneities. It is well known that dispersivities are scale dependant (Dagan, 1989; Gelhar et al., 1992; Hiscock, 2005). Based on the lower limit for dispersivity, the cell Peclet number <2 (Voss and Provost, 2003), and a reasonable computation time, $\alpha_L = 15$ and $\alpha_T = 1.5$ were used to account for all heterogeneity on the scale of the model. The large number of nodes was the decisive factor in determining computation time, while temporal refinement was less important. A time step of one month was used for a total simulation period of 10,058 years, which contributed to decreased oscillation, improved accuracy and decreased numerical dispersion. Mixing effects caused by tidal movements are accounted for by the dispersivity values applied.

Transient simulations for various choices of model parameters (Table 1) were run for the model set-up presented in this study. The results indicate that a time span of ∼800 years was enough for the position of the transition zone to reach equilibrium with present sea level. To calibrate the steady state model, an analytical solution based on average piezometric heads measured in 2003–2005, and the Ghyben–Herzberg relation (Ghyben (1888) and Herzberg (1901)) was used. Unfortunately, earlier studies in the same area (Muianga, 1992) were not of the quality needed for calibration purposes.

Discussion of the sensitivity to the different parameters is based on simulations run to "steady state" condition. A simulation time of 3000 years was assumed sufficient to reach "steady state" conditions, because the position of the interface changed less than 0.01 m and the thickness of the transition zone changed approximately 0.01 m in the last 100 years of the simulation.

The best fit of the steady state situation was determined by comparing it with the analytical solution for the present vertical position of the salt–fresh interface. This solution is based on measurements of groundwater heads. The best fit was obtained for the combination of parameters listed in Table 2 (Fig. 4).

4. Results

Regardless of the parameter values applied, steady state conditions are obtained faster closer to the discharge boundary for both the interface position and the transition zone thickness (Fig. 5a). The transition zone thickness calculated along vertical lines in the model domain increases from the centre outwards and then decreases towards the discharge boundaries (Fig. 4).

The sensitivity of the interface position and thickness of the transition zone to changes in parameter values are shown in Table 3. A change in vertical permeability does not affect the interface position or the time it takes to reach steady state (Fig. 5b), while lower horizontal permeability causes a downward shift and increases the time to reach steady state (Fig. 5c). The interface position also displays sensitivity to recharge. Increased recharge moves the interface downwards and steady state is reached faster for a higher recharge rate compared to lower recharge rates (Fig. 5d). Neither porosity, nor dispersivity affects the interface position (Fig. 5e and f respectively). However, unlike other parameters, dispersivity strongly affects the thickness of the transition zone (Fig. 5f). As soon as the vertical movement rate diminishes, the thickness of the transition zone moves towards equilibrium. The equilibrium is first reached close to the boundary and later further away (see Fig. 5a). These results are in line with the results obtained by Eeman et al. (2011) for rain water lenses on a much smaller scale.

In the early phase of the transient simulation towards a steady state situation the flow is dominantly vertical almost everywhere as the interface is replaced. In this phase longitudinal dispersion causes the mixing, and hence the transition zone. This is in agreement with the conclusion by Kiro et al. (2008), stating that longitudinal dispersivity causes a widening of the transition zone as the transition zone moves vertically during a change in base level.
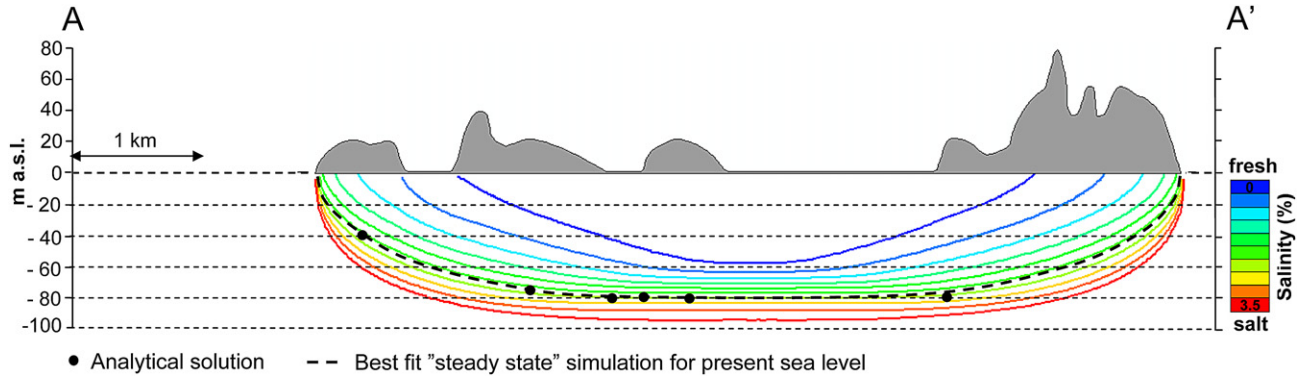
Fig. 4. The best simulated fit to analytical solution for the vertical position of the salt–fresh interface. The analytical solution is based on average piezometric heads measured in 2003–2005, and the Ghyben–Herzberg relation (Ghyben (1888) and Herzberg (1901)), and was obtained for the set of parameters listed in Table 2.
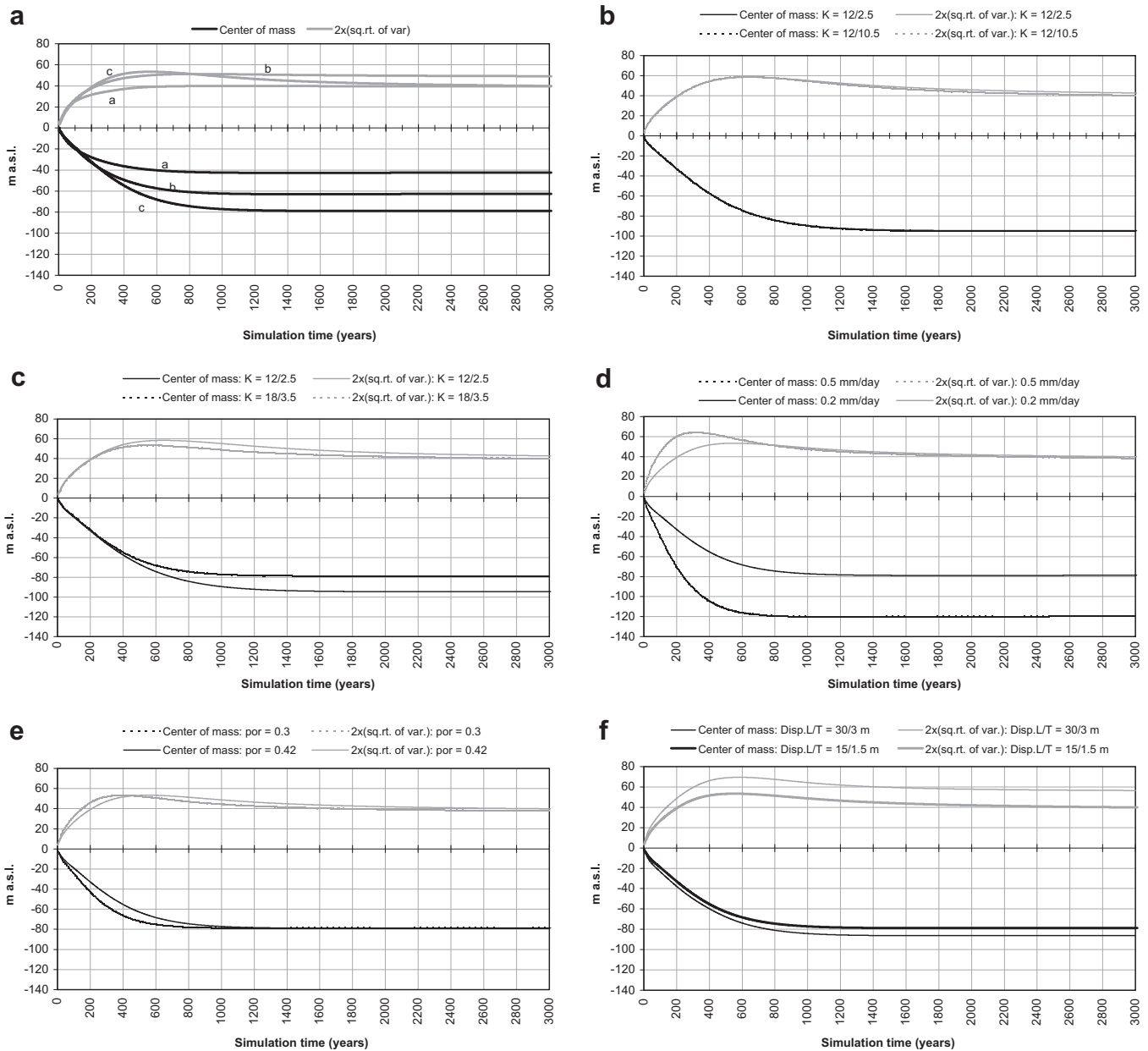

Fig. 5. Plot of spatial statistical moments of the concentration field along lines a, b and c in Fig. 3 along which spatial statistical moments have been calculated, illustrating the effects of a) distance to the specified head boundary, b) variable vertical hydraulic conductivity, c) variable horizontal hydraulic conductivity, d) variable recharge rate, e) variable porosity, f) variable dispersivity. For Fig. 5b–f the results are only shown for line c in Fig. 3.

Table 3
Changes in parameter value input to the model and the effects on simulated interface position, lens thickness, and response time. Only one parameter has been changed at the time compared to Table 2 if nothing else is stated.

Parameter	Value change	Change in interface position (m)	Change in lens thickness (m)	Time to reach SS for interface position
Recharge	0.0002 → 0.0005 (m/day)	−∼40	−∼1.5	faster
K_{hor}/K_{ver}	18/3.5 → 12/2.5 (m/day)	−∼16	+∼3	slower
K_{hor}/K_{ver}	12/2.5 → 12/10.5 (m/day)	none	−∼1.5	no difference
Porosity	0.42 → 0.30	none	−∼2.5	faster
α_L/α_T	15/1.5 → 30/3 (m)	none	+∼16	no difference

Later in the simulation, the flow is almost parallel to the interface, in which case the smaller transversal dispersion takes over, causing less mixing. For this reason there is an increase in the thickness of the transition zone, followed by a decrease (Fig. 5 a–f). This is in line with the findings of Eeman et al. (2011). Another contributing factor to the spatial distribution of the interface is that the vertical line, along which spatial statistics are calculated, is perpendicular to the interface in the centre of the domain, while this is not the case close to the seepage boundaries. Also, converging streamlines close to the seepage boundaries influence the thickness of the transition zone close to these boundaries (Eeman et al., 2011).

If the sea-level curve established by Ramsay (1995) is correct Inhaca was split into several smaller islands in parts of the Middle and Late Holocene, each developing separate freshwater lenses (Fig. 6). Along the cross-section A–A′ (see Fig. 1) four smaller "islands" are indicated, ranging in width from 600 to 1800 m, as opposed to the present single island. The transient calculations seen in Fig. 7 are done in the centre of the domain (C in Fig. 3) which represents the transition from one big island (∼7000 m across) to several smaller islands, and vice versa, as sea-level rises above or drops below the set flooding threshold of the central low-lying areas. The timing of the shift in node condition (pressure vs. source of fluid) is driven by the changing sea level according to the sea-level curve constructed by Ramsay (1995) (Fig. 2).

5. Discussion

The response times (hundreds of years) in the salt–fresh groundwater system of Inhaca are affected by horizontal permeability, recharge rate, and porosity. A higher permeability allows for a greater flux of water, and thereby shorter response times (Fig. 5c). Similarly, but on a considerably shorter time scale (hours), Underwood et al. (1992) showed response time to tidal variations to be shorter for higher permeability values in their study of small (250 m–1000 m in width) atoll islands. A faster pore flow is needed to account for a higher recharge rate; hence response time becomes shorter (Fig. 5d). The opposite effect is seen for an increased

porosity due to the ability to store greater volumes of water (Fig. 5e).

In their study of the lens dynamics of atoll islands Underwood et al. (1992) concluded that the position of the salt/fresh interface is not very sensitive to tidal movement. Therefore, the use of a non-tidal model is considered adequate to study response times, and variations in the interface position during the Holocene. Underwood et al. (1992) also regarded tidal movement to be decisive for the mixing process in the transition zone, and used responses to tidal variations in the transition zone for calibration. However, the island they studied was considerably smaller than Inhaca and in this case the tidal effect plays a smaller role. The length of the time steps used in this study is much longer (1 month) than tidal movement. A similar calibration therefore would have become meaningless, and transient calibration would in general have been difficult due to lack of control data.

The development of a freshwater lens is considerably faster in the early phase of the process than in the late phase (Fig. 5 a–f), i.e. the freshening process goes more slowly as the position of the transition zone moves towards equilibrium with the given sea level. The main factors that are decisive for the vertical positioning of the salt–fresh interface are horizontal permeability (Fig. 5c) and total recharge. The latter is a function of the recharge rate (Fig. 5d) and recharge area (here: island size) (Fig. 7). Also, as demonstrated by Yechieli et al. (2010), a low-angle coastal topography, which particularly is the case for the Maputo Bay on the western side of Inhaca (see Fig. 2), will have a greater inland shift of the interface position due to sea-level change compared to a steep coastal topography. Underwood et al. (1992) found that the ability to form a lens of fresh water under atoll islands depended on the relationship between island widths and recharge rate. Generally, for the smaller islands a greater recharge rate was needed to form a lens of potable water. For Inhaca the split into four smaller islands would have meant a great reduction in the volume of fresh water.

The simulation in Fig. 7 shows repeating freshening and salinization processes during the Holocene in response to varying sea level, indicating response times of a few centuries. Similar response
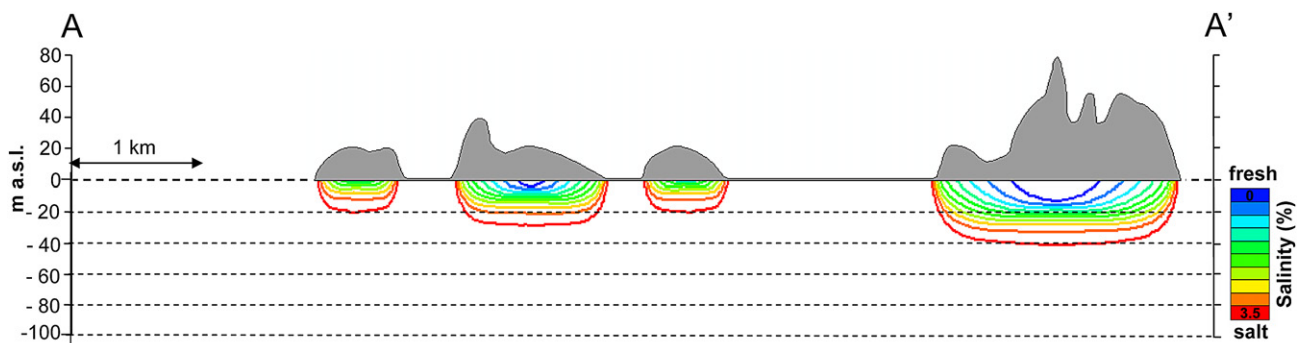

Fig. 6. The development of multiple groundwater lenses along line A–A′ (Fig. 1) during Holocene sea-level high stands.
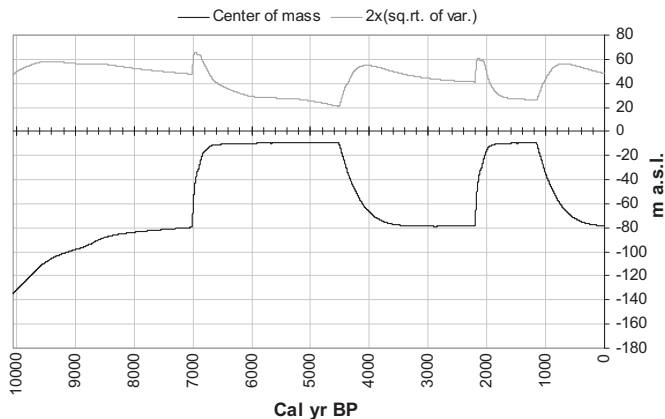
Fig. 7. Plot of spatial statistical moments of the concentration field along line c in Fig. 3 illustrating the Holocene dynamics of the salt–fresh groundwater interface under Inhaca Island. In this case it illustrates the effect of changing the configuration from a big island to a considerably smaller island.

times were found by Lambrakis and Kallergis (2001) and Lambrakis (2006) in their studies of freshening times of saline coastal aquifers in Greece.

Steady state simulations indicate that for an initial recharge of 0.2 mm/day (8% of MAP) a ±10% change in recharge rate will cause a vertical shift in the interface position of ±4 m. The steady state simulation was done for present sea level, hence one island. As both sea-level rise and wetter than present conditions are associated with warmer climate during the Holocene it is likely that a +10% recharge rate will occur at a time when the recharge area of Inhaca was considerably smaller than today. Hence, the effect of an increased recharge rate of 10% would have been negligible for the position of the interface compared to the impact of reduced recharge area. The same applies to the period of sea-level rise prior to 7000 cal BP. The most recent drier than present period was the Little Ice Age (700–200 cal BP). Decreased recharge in this period would have lifted the interface, but the effect is likely to have been small compared to earlier Holocene fluctuations. Thus the Holocene switches from terrestrial to marine back to terrestrial conditions, are believed to have effected the interface position much more than did the variations in rainfall.

In their study of the effects of large scale sea-level fluctuations on the seawater–freshwater interface in the northern Atlantic Coastal Plain Meisler et al. (1984) concluded that the salt–fresh interface is not in equilibrium with present sea level. This is in agreement with the conclusion by Essink (1996) that a time lag between cause and effect explains why the present groundwater flow regime along the Dutch coast is not yet in equilibrium. Essink (1996) further found that small hydrogeologic systems (<10 km), with sea on both sides of the system, are highly sensitive to sea-level variations and that a time lag between cause and effect can be expected to be a few centuries for such systems. The transient simulations for Inhaca are in agreement with this time-lag estimate.

According to the curve presented by Ramsay (1995) the sea level along the southeast coast of Africa has been stable at the present level for the past ∼800 years, and the response times seen in the transient simulations (Fig. 7) show that the assumption of interface equilibrium with present sea level is reasonable for Inhaca, given the conceptual model presented. However, it is acknowledged that the conceptual model is likely to be over-simplified due to a lack of geologic and hydrologic information. The numerical simulations demonstrate that a higher permeability would give an elevated transition zone (Fig. 5c) closer to the results interpreted from Muianga (1992). The model is nevertheless regarded as adequate to

study the effects of the parameters considered in this study on the transition zone position and mixing processes.

Great changes in the freshwater resources may also take place in the future. With the worst case scenario for sea-level rise of ∼0.6 m/century (IPCC, 2007) a similar flooding of the central parts of Inhaca may take place within just two centuries. However, negative effects of an increased sea-level may take place even earlier as the seawater at high tide is already close to a critical elevation. As tidal channels expand and become progressively more permanent this could have grave effects on the island's freshwater resources. The implications for the inhabitants could be devastating as a major part of their cultivated land may be inundated by seawater. The central areas of Inhaca constitute the greatest storage of fresh groundwater today, with >60 m depth of potable water. Many of the present drinking water wells close to the wetlands will be at risk of seawater intrusion and undrinkable in less than two centuries. Of more immediate concern, however, is the potential development of large scale tourist industry with a high demand for water resulting in over-consumption followed by salt-water intrusion. As seen from the studies by Lambrakis and Kallergis (2001) and Lambrakis (2006) freshening time may be considerable.

6. Conclusions

The adapted version of SUTRA has proven useful for studying the effects of dynamic changes in the salt–fresh groundwater interface in response to sea-level fluctuations, i.e. the boundary condition is related to the time-dependent sea level. The calculation of spatial statistical moments of the concentration field provides the opportunity to characterize the transition zone over time, and to illustrate and compare the results.

The response time is sensitive to porosity, hydraulic conductivity and recharge. Reduced porosity, increased hydraulic conductivity, and increased recharge rate all reduce the response time, while dispersivity has no effect. Interface position is determined by the recharge rate and the hydraulic conductivity, while the thickness of the transition zone in this non-tidal model is controlled by the dispersivity values applied.

The transient model reflects the concept of a changing boundary configuration as a response to fluctuating Holocene sea level, i.e. moving from a one-island concept, as seen today, to a multi-island concept during sea-level high stands. The thickness of the transition zone is affected by the vertical movement, and is reduced during periods of stability. In the multi-island setting the total recharge area is dramatically reduced, and so is the volume of fresh water. The effects on future water supply could therefore become severe where existing coastal aquifers run the risk of fragmentation due to sea-level rise.

The geomorphologic and hydrogeologic setting seen at Inhaca Island is not believed to be unique, and so the knowledge of this setting, along with responses to changes in the past, need to be taken into consideration when establishing future management plans for coastal aquifers.

Soil Physics, Ecohydrology and Groundwater Management Group at the Wageningen University for their kind hospitality and valuable input to the modelling work.

References

Bredenkamp, D.B., Botha, L.J., Venter, D., 1993. St Lucia Lake: geohydrology and related aspects. In: Taylor, R.H. (Ed.), Proceedings of the Workshop on Water Requirements for Lake St Lucia. Fanies Island 12 & 13 May 1992. Department of Environment Affairs, Pretoria, South Africa.

Cuamba, F., Stabell, B., Haldorsen, S., Achimo, M., Mugabe, J., Været, L., 2007. The late Holocene evolution of the tropical Island of Inhaca, Mozambique. Quaternary International 167–168, 84–85.

Dagan, G., 1989. Flow and Transport in Porous Formations. Springer Verlag, Heidelberg.

Direcção Nacional de Geologia de Moçambique, 1995. Série Geológica 1:50 000, Folha N°2532D3.

Eeman, S., Leijnse, A., Raats, P.A.C., van der Zee, S.E.A.T.M., 2011. Analysis of the thickness of a fresh water lens and of the transition zone between this lens and upwelling saline water. Advances in Water Resources 34, 291–302.

Essink G.H.P.O., 1996. Impact of sea level rise on groundwater flow regimes: a sensitivity analysis for the Netherlands. PhD-thesis. Technische Universiteit Delft, The Netherlands.

Essink, G.H.P.O., 2001. Improving fresh groundwater supply – problems and solutions. Ocean and Coastal Management 44, 429–449.

Fish, J.E., 1988. Hydrogeology, Aquifer Characteristics, and Ground-Water Flow of the Surficial Aquifer System. U.S. Geological Survey, Broward County, Florida. Water Resources Investigations Report 87-4034.

Fish, J.E., Stewart, M., 1991. Hydrogeology of the Surficial Aquifer System, Dade County. U.S. Geological Survey, Florida. Water Resources Investigations Report 90-4108.

Fleming, K., Johnston, P., Zwartz, D., Yokoyama, Y., Lambeck, K., Chappell, J., 1998. Refining the eustatic sea-level curve since the Last Glacial Maximum using far- and intermediate-field sites. Earth and Planetary Science Letter 163, 327–342.

Gelhar, L.W., Welty, C., Rehfeldt, K.R., 1992. A critical review of data on field-scale dispersion in aquifers. Water Resources Research 28, 1955–1974.

Ghyben, W.B., 1888. Nota in Verband Met de Voorgenomen Putboring Nabij Amsterdam. Tijdschrift Van Let Koninklijk Inst. Van Ing.. as cited in Freeze, R.A., Cherry, J.A., 1979.

Govindaraju, R.S., Das, B.M., 2007. Moment Analysis for Subsurface Hydrologic Applications. Water Science and Technology Library, vol. 61. Springer Verlag, Dordrecht.

Hazen, A., 1911. Discussion: dams on sand foundations. Transaction American Society of Civil Engineers 73, 199.

Herzberg, A., 1901. Die Wasserversorgung einiger Nordseebader. Journal Gasbeleuchtung und Wasserversorgung 44 (815–819), 842–844.

Hiscock, K.M., 2005. Hydrogeology: Principles and Practice. Blackwell Publishing, Malden.

Hobday, D.K., 1977. Late Quaternary sedimentary history of Inhaca Island, Mozambique. Transaction of the Geological Society of South Africa 80, 183–191.

Holmgren, K., Lee-Thorp, J.A., Cooper, G.R.J., Lundblad, K., Partridge, T.C., Scott, L., 2003. Persistent millennial-scale climatic variability over the past 25,000 years in Southern Africa. Quaternary Science Reviews 22, 2311–2326.

IPCC, 2007. Climate change 2007: the physical science basis. In: Solomon, S., Qin, D., Manning, M., Chen, Z., Marquis, M., Averyt, K.B., Tignor, M., Miller, H.L. (Eds.), Contribution of Working Group I to the Fourth Assessment Report of the Intergovernmental Panel on Climate Change. Cambridge University Press, Cambridge, United Kingdom and New York, NY.

Kalk, M., 1995. A Natural History of Inhaca Island, Mozambique, third ed. Witwatersrand University Press, Johannesburg, South Africa.

Kiro, Y., Yechieli, Y., Lyakhosky, V., Shalev, E., Starisky, A., 2008. Time response of the water table and saltwater transition zone to the base level drop. Water Resources Research 44, W12442.

Kooi, H., Groen, J., Leijnse, A., 2000. Modes of seawater intrusion during transgressions. Water Resources Research 36, 3581–3589.

Lambeck, K., Chappell, J., 2001. Sea level change through the last glacial cycle. Science 292, 679–686.

Lambeck, K., Esat, T.M., Potter, E.K., 2002. Links between climate and sea levels for the past three million years. Nature 419, 199–206.

Lambrakis, N., 2006. Multicomponent heterovalent chromatography in aquifers. Modelling salinization and freshening phenomena in field conditions. Journal of Hydrology 323, 230–243.

Lambrakis, N., Kallergis, G., 2001. Reaction of subsurface coastal aquifers to climate and land use changes in Greece: modeling of groundwater refreshening patterns under natural recharge conditions. Journal of Hydrology 245, 19–31.

Meisler, H., Leahy, P.P., Knobel, L.L., 1984. Effects of Eustatic Sea-level Changes on Saltwater–freshwater in the Northern Atlantic Coastal Plain. Geological Survey water-supply paper; 2255 USGS, Alexandria, USA.

Meyer, R., Godfrey, L., 1995. Characterization and Mapping of the Groundwater Resources, Kwazulu-Natal Province. Mapping Unit 7. Directorate of Geohydrology. Department of Water Affairs and Forestry, Pretoria, South Africa.

Ministério de Defesa Nacional, 1985. Do Cabo Inhaca a Ponta Vermelha 46660-M, 1:50,000.

Muianga, A., 1992. Estudo hidrogeológico da parte ocidental da Ilha da Inhaca. Licenciatura Department of Geology. University of Eduardo Mondlane, Mozambique.

Partridge, T.C., 1997. Cainozoic environmental change in southern Africa, with special emphasis on the last 200 000 years. Progress in Physical Geography 21, 3–22.

Partridge, T.C., Scott, L., Hamilton, J.E., 1999. Synthetic reconstructions of southern African environments during the Last Glacial Maximum (21–18 kyr) and the Holocene Altithermal (8–6 kyr). Quaternary International 57-58, 207–214.

Peltier, W.R., 2002. On eustatic sea level history: Last Glacial Maximum to Holocene. Quaternary Science Reviews 21, 377–396.

Ramsay, P.J., 1995. 9000 years of sea-level change along the southern African coastline. Quaternary International 31, 71–75.

Ramsay, P.J., Cooper, J.A.G., 2002. Late Quaternary sea-level change in South Africa. Quaternary Research 57, 82–90.

Schwartz, F.W., Zhang, H., 2003. Fundamentals of Groundwater. John Wiley & Sons, Inc., New York.

Scott, L., Lee-Thorp, J.A., 2004. Holocene climate trends and rythms in southern Africa. In: Battarbee, R.W., Gasse, F., Stickley, C.E. (Eds.), Past Climate Variability Through Europe and Africa. Springer, Dodrecht, The Netherlands, pp. 69–95.

Sénvano, A., Rebêlo, L., Marques, J., 1997. Notícia Explicativa da Carta Geológica da Ilha da Inhaca. Mozambique, Direcção Nacional de Geologia, Ministério dos Recursos Minerais e Energia. 1/25,000.

Tyson, P.D., 1999. Atmospheric circulation changes and palaeoclimates of southern Africa. South African Journal of Science 95, 194–201.

Tyson, P.D., Partridge, T.C., 2000. Evolution of Cenozoic Climates. In: Partridge, T.C., Maud, R.R. (Eds.), The Cenozoic of Southern Africa. Oxford Monographs on Geology, vol. 40 (23), 371–387.

Underwood, M.R., Peterson, F.L., Voss, C.I., 1992. Groundwater lens dynamics of atoll islands. Water Resources Research 28, 2889–2902.

Voss, C.I., Provost, A.M., 2003. SUTRA – A Model for Saturated-Unsaturated Variable-Density Ground-Water Flow with Solute or Energy Transport. U.S. Geological Survey Water-Resources Investigations, Report 02-4231, 260 pp. http://water.usgs.gov/nrp/gwsoftware/sutra/SUTRA_2D3D_1-documentation.pdf Cited 15 Aug 2008.

Winston, R.B., Voss, C.I., 2004. SutraGUI: A Graphical User Interface for SUTRA, A Model for Ground-Water Flow with Solute or Energy Transport U.S. Geological Survey Open-File Report 03-285.

Yechieli, Y., Shalev, E., Wollman, S., Kiro, Y., Kafri, U., 2010. Response of the Mediterranean and Dead Sea coastal aquifers to sea level variations. Water Resources Research 46, W12550.